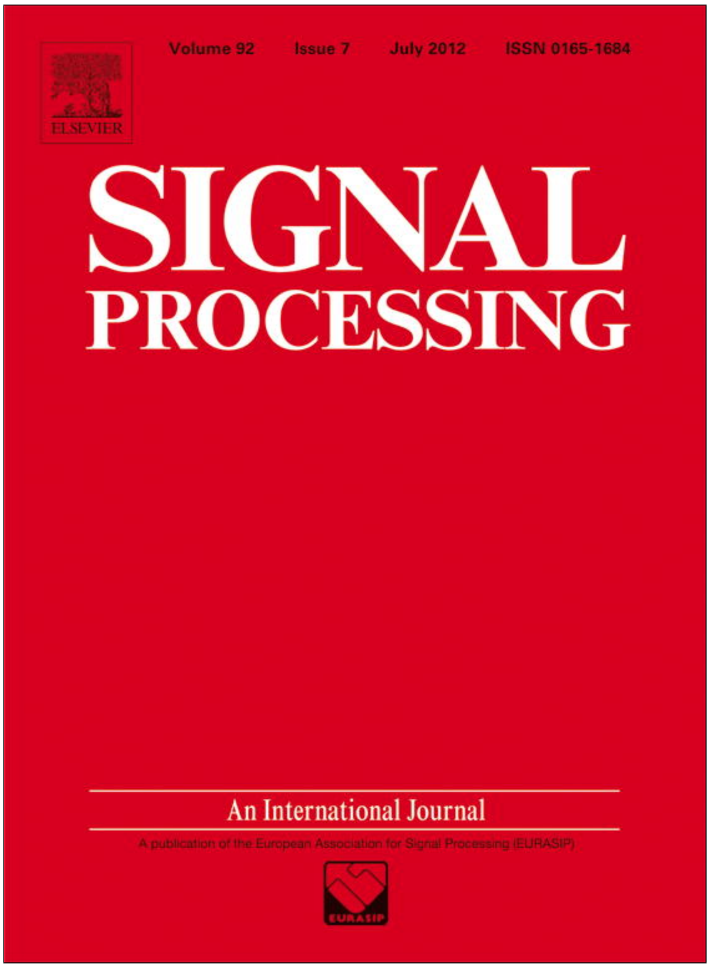
Volume 92 Issue 7 July 2012 ISSN 0165-1684
ELSEVIER
SIGNAL
PROCESSING
An International Journal
A publication of the European Association for Signal Processing (EURASIP)
EURASIP

Signal Processing 92 (2012) 1567–1579

Contents lists available at SciVerse ScienceDirect

Signal Processing

journal homepage: www.elsevier.com/locate/sigpro

Strongly concave star-shaped contour characterization by algebra tools

Haiping Jiang, Julien Marot, Caroline Fossati, Salah Bourennane *

GSM Group, Institut Fresnel, Ecole Centrale Marseille D.U. de Saint Jérôme Av. Escadrille Normandie, 13397 Marseille, France

ARTICLE INFO

Article history:
Received 22 April 2011
Received in revised form
22 September 2011
Accepted 3 October 2011
Available online 14 January 2012

Keywords:
Contour
Concavity
Array
Damped sinusoid
Estimation

ABSTRACT

In this paper, we discuss the problem of recovering a star-shaped contour with the assumption that the contour coordinates can be decomposed into damped sinusoids. We propose a signal generation method derived from the array processing paradigm, which yields the center and radius of a circle fitting the contour. Starting from an initialization circle, we propose to estimate the oscillations of the expected contour around this circle with a method which copes with noise and strong concavities. We adopt a signal characterization method which provides the parameters of damped sinusoids. In addition, we propose a refinement step based on an optimization method which improves the adequation of the collected signals to the proposed model. The novel proposed method is compared with an approach based on signal generation and gradient optimization method, and with GVF method. The experiments show that the proposed method offers a significant improvement in terms of pixel bias and computational load, in particular when strongly concave contours in noisy images are considered. Moreover, the computational load of the proposed method is independent from the contour concavity and the noise level.

1. Introduction

Numerous edge detection methods have been proposed. Examples of edge detectors are operators that incorporate linear filtering [1,2], or local energy [3]. Other more original edge detection tools include anisotropic diffusion [4]. We can distinguish two categories of edge detection methods: region-based methods and contour-based methods. We will confine our exposition to a partial list of contour-based methods: the Hough transform is originally meant for the retrieval of straight lines. Its generalized version (GHT) [5] retrieves the center of multiple circles, knowing their radius. A well-known limitation of the Hough transform is its elevated computational load, which dramatically increases when the number of noise pixels increases. GHT is robust to partial or slightly deformed shapes and tolerant to noise in terms of estimation accuracy, but GHT requires a high computational load and a huge storage space, in particular when the number of noise pixels increases. Level Set segmentation relies on active contours and techniques of curve evolution [6]. To avoid some irregularities in the active contour evolution, a recent improved version [7] proposes a new variational Level Set formulation in which the regularity of the Level Set function is intrinsically maintained during the Level Set evolution. A drawback of the Level Set approach is still the tuning of numerous parameters. Gradient Vector Flow (GVF) [8] retrieves concavities and weak edges with blurred boundaries. GVF limitations can be observed when the expected contour exhibits a strong concavity, that is, a strong curvature: it was then improved to handle concave regions [9].

Still in the frame of contour-based methods, it has been proved that array processing and frequency retrieval

* Corresponding author.
E-mail address: salah.bourennane@fresnel.fr (S. Bourennane).

0165-1684/$ - see front matter © 2011 Elsevier B.V. All rights reserved.
doi:10.1016/j.sigpro.2011.10.002

are profitable to image segmentation, either by a region-based approach [10]or a contour-based approach [11–13]. Array processing and frequency retrieval are based on algebra tools. They rely in particular on subspace approaches [14] to retrieve source parameters such as direction of arrival (DOA) [15,16]. These subspace-based methods have been recently improved in terms of computational load by avoiding eigendecomposition [17,18]. Algebraic subspace-methods are also used for frequency estimation purposes [19–23]. Algebraic methods coming from array processing have been transposed to image segmentation. In [10], a region approach is adopted. The authors present a sensor array processing approach to detect the number of object regions. This number provides the necessary information for unsupervised image segmentation. In [11–13], a contour based approach is adopted, and particular features are expected: either polygons [11], straight lines [12], or circles [13].

Firstly, in [11], binary polygons can be reconstructed from a finite number of their complex moments. As pointed out, the formulation of the shape-from-moments problem is very similar to several other fields, such as estimation of sinusoidal component in speech signal processing [22], and of direction of arrival in array processing [24,25]. In a noisy case, the contour reconstruction issue becomes an estimation one. The recovered binary polygonal vertices are refined by generalized pencil of function, Hankel total least squares method and structured total least squares method. Other numerical procedures are presented for the shape-from-moments reconstruction problem in [26,27]. It turns out that all of these have established the explicit connection between the binary polygonal object reconstruction problem and the field of array processing.

Secondly, a similar analogy is made in [12] between a straight line in an image and a planar propagating wavefront impinging on an array of sensors to obtain an array processing formulation for the detection of line parameters within an image, replacing the classic Hough transform approach.

Thirdly, several extensions of this analogy have been developed to recover linear [28,29], triangular [30], and circular contours [13,31]. Especially, a different signal generation scheme is proposed in [13], which yields an array processing linear phase signal model out of a binary image containing a circle. In the linear and circular cases, high resolution methods [24,25] could then be applied to distinguish possibly very close contours by considering them as punctual sources.

There exist limitations to these array processing-based methods. One drawback is that they are limited to relatively simple shapes: either lines [12,28], possibly slightly distorted circles [13], or polygons with three or four corners [11]. And another drawback is that these methods are limited to a low-noise environment.

The main contributions of this paper are as follows:

Firstly, we detect star-shaped contours which may exhibit strong concavity. For this, we detect blindly the center of gravity of the contour [13] and choose an adequate system of polar coordinates which permits to consider the contour as star-shaped. Getting inspired from an existing signal generation method [13], we transform the content of the data composed of a 2-D image into a 1-D signal. The obtained signal contains the information of the contour radial coordinates. Contrary to what has been done in previous works, the contour is no longer supposed to be linear, circular, or polygonal. It only has to be star-shaped. We assume that the polar coordinates of a closed circular-like contour edge is the sum of several damped sinusoidal components. In this way, the problem of edge characterization is transformed into the estimation of the amplitude, frequency, and damping factor of each sinusoidal component. In this way, we are able to characterize entirely the contour coordinates with a parametric estimation method of multiple damped sinusoids [23]. The advantage of using a parametric method is that the computational load is independent from the parameter values. In particular, we may retrieve very concave contours if the frequency and the amplitude values are sufficiently elevated.

Secondly, we take into account the requirements of the frequency estimation method about the algebraic structure of the signal generated out of the image: the generated signal must be refined to fit the model required for the damped frequency estimation. For this, we rearrange the data as a Hankel matrix form, and we refine the signal by solving a so-called Structured Total Least Norm (STLN) problem [32], to get a processed matrix which is rank deficient. This process is necessary only in the case of high noise, where it slightly decreases the bias between expected and estimated contours.

The outline of the paper is as follows. In Section 2, we describe the problem of retrieving a star-shaped contour, and show that an adequate image transformation process permits to reformulate this problem as a damped exponential sinusoidal model. In Section 3, parameter estimation based on the damped exponential sinusoid model is exploited. In Section 4, the generated signals are refined to compensate the presence of noise. In Section 5, experiments are performed which show that our method offers an improvement in terms of pixel bias and computational load, in particular when strongly concave contours in noisy images are considered.

The proposed method is compared with GHT [5], with an array processing-based method [13] which adapts gradient descent, and with GVF [8].

2. Problem overview and formulation

In this section, we overview the problem of retrieving a circular contour. Then we focus on the more general case of a star-shaped contour and formulate the problem that we solve in this paper. Our framework is that of parameterized object-based geometric reconstruction, as opposed to pixel-to-pixel local methods such as GVF [8].

2.1. Problem overview

Assume that a closed circular contour is in an $N \times N$ recorded image $I_{l,m}$ (see Fig. 1). The most simple star-shaped contour is the circle. A circle is supposed to have center coordinates (l_c, m_c) and radius r. Note that, for a

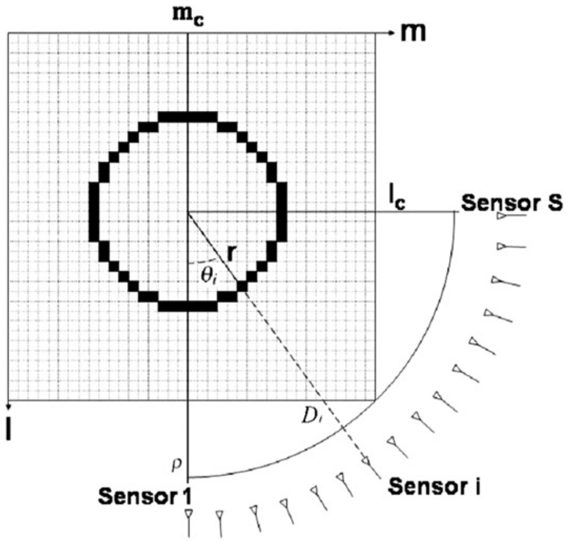

Fig. 1. Circular contour with center (l_c,m_c), array compound of S sensors, example of direction for signal generation D_i.

binary image, $I_{l,m}=1$ on the contour and $I_{l,m}=0$ otherwise. We propose to generate a one-dimensional signal out of the two-dimensional image, and to exploit this signal to get the radial coordinates of the expected contour. For this, we get inspired from [13]: a circular array of sensors is associated with the image. The sensor array is supposed to be placed along a quarter of circle centered on the center point of the expected circle. Let D_i be the line that makes an angle θ_i with the vertical axis, as shown in Fig. 1. A signal component z_i is associated with each signal generation D_i. The signal component z_i for a given sensor i is generated starting from the top left corner of the sub-image, and ending on the sensor i. Each sensor receives the signals only along its corresponding direction from center to sensor. All pixels in the image are assumed to propagate narrow-band electromagnetic waves with zero initial phases. Furthermore, the waves emanating from pixels in a given direction are confined to travel only along this direction and towards the corresponding sensor. For more details, refer to [12,13]. The signal component for a given sensor i is generated by the pixels in every D_i direction as follows:

$$z_i=\sum_{l=1}^{N_s}\sum_{\substack{m=1\\(l,m)\in D_i}}^{N_s} I_{l,m}\sqrt{l^2+m^2},\quad i=1,\ldots,S \tag{1}$$

where N_s is the maximum number of rows and columns in the sub-image. The signal components form the signal vector $\mathbf{z}=[z_1,z_2,\ldots,z_S]^T$, where $(\cdot)^T$ denotes matrix transposition.

The considered signal generation process requires the knowledge of the center coordinates (l_c,m_c). To estimate them, a linear array of sensor is placed along the left (or bottom) side of the image [12,28], and the following signal generation schemes can be adopted: $z_l^{left}=\sum_{m=1}^{N} I_{l,m},\quad l=1,\ldots,N$ and $z_m^{bottom}=\sum_{l=1}^{N} I_{l,m},\quad m=1,\ldots,N$. These signal components form the vectors $\mathbf{z}^{left}=[z_1^{left},\ldots,z_N^{left}]^T$ and $\mathbf{z}^{bottom}=[z_1^{bottom},\ldots,z_N^{bottom}]^T$. By detecting the dominant components in signals $\mathbf{z}^{left}$ and $\mathbf{z}^{bottom}$, we can compute the center coordinates, with a method similar to [13]. There exist some other methods, such as the extension of the Hough transform [5], and the least squares method [33] to find the center coordinates of a circle.

When a single one-pixel wide circular contour with radius r is present, the signal components read

$$z_i=r,\quad i=1,\ldots,S \tag{2}$$

The radius value can be estimated as

$$r=\overline{z} \tag{3}$$

where $\overline{z}$ is defined as: $\overline{z}=(1/S)\sum_{i=1}^{S} z_i$.

We now consider the more general case of any star-shaped contour in a noisy environment. The contour radial coordinates are contained in the vector $\rho=[\rho_1,\rho_2,\ldots,\rho_Q]^T$, where $Q=4S-1$. To retrieve all contour coordinates, we need as many sensors as contour coordinates. Therefore, we associate the image with a circular antenna which surrounds the whole image and is compound of Q sensors. The maximum radius of a circle centered on the center of the image is $N/2$, and one quarter of this circle is made of approximately $\sqrt{2}*(N/2)$ pixels. For an exhaustive characterization of the contour, each pixel must be associated with a sensor. So for the whole image the minimum number of sensors Q is such that: $Q\geq 2\sqrt{2}*N$. For a highly concave contour, a higher number of sensors will be necessary to characterize all contour pixels. An example of contour and this antenna are represented on Fig. 2.

When any one-pixel wide star-shaped contour is present, the signal components read

$$z_i=\rho_i+n_i,\quad i=1,\ldots,Q \tag{4}$$

where n_i is a noise term originated by the noise pixels. Note that the signal generation process is simplified compared to the one proposed in [13]: no propagation constant is used, and signal components are directly related to the contour coordinates. This simplification is permitted because a single contour is expected.

We express the radial coordinates as

$$\rho_i=r+x_i,\quad i=1,\ldots,Q \tag{5}$$

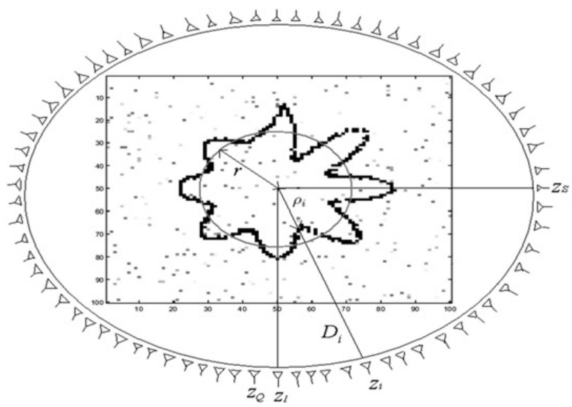

Fig. 2. Star-shaped contour with coordinates $\rho_i,\quad i=1,\ldots,Q$, fitting circle with radius r, array of Q sensors, example of direction for signal generation D_i, generated signal components $z_i,\quad i=1,\ldots,Q$.

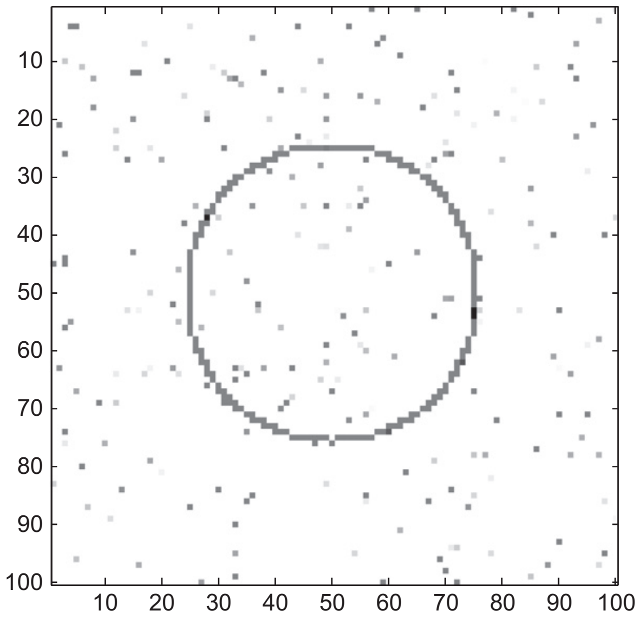

Fig. 3. Circle: processed image.

where x_i is the oscillation of the ith pixel around the circle of radius r (see Fig. 2). Therefore, the generated signal of Eq. (4) now can be reformulated as

$$z_i = r + x_i + n_i, \quad i = 1, \ldots, Q \tag{6}$$

To characterize entirely the expected contour, it is necessary to retrieve, from the signal components z_i, $i=1, \ldots, Q$, the parameters r and x_i, $i = 1, \ldots, Q$. Existing methods such as least squares [34], or Gradient descent [13] could be adapted for this purpose. Snakes methods such as GVF [8] can retrieve closed contours in a noisy environment. However, least squares are sensitive to noise, and the two other methods exhibit drawbacks which will be demonstrated in the result section. That is why we formulate the problem in a different, novel way.

2.2. Problem formulation

From the signals $\mathbf{z} = [z_1, z_2, \ldots, z_Q]^T$ of Eq. (6), we wish to retrieve the radius value r, and the oscillations x_i, $i = 1, \ldots, Q$, in particular from contours presenting a strong concavity. Without loss of generality, we define r as the mean value of the components z_i $i = 1, \ldots, Q$. r is estimated as

$$r = \overline{z} \tag{7}$$

Then, we can compute

$$x_i = z_i - r, \quad i = 1, \ldots, Q \tag{8}$$

The values x_i, $i = 1, \cdots, Q$ are exactly the edge oscillation values in the case where the image is not impaired with noise. If the image is impaired with uniformly distributed noise, the computation of Eq. (8) provides signal components x_i, $i = 1, \ldots, Q$, which are impaired by random noise, due to the influence of random noise pixels on the signal generation process. Therefore, we seek for a method which retrieves the oscillations of possibly strongly concave contours, and which is robust to noise. For this, we propose in the next subsection a model for edge oscillations x_i, $i = 1, \ldots, Q$. We will further adapt an advanced damped frequency retrieval method to characterize the edge oscillations, in accordance with the proposed model.

2.3. Damped sinusoidal model for edge oscillations

For the edge oscillations of a star-shaped contour, the pixel coordinates in a polar representation are supposed to follow a generalized version of the sinusoidal model, that is, K damped sinusoidal components, each of which has respective amplitude, frequency and damping factor. So we model the edge oscillations as follows:

$$x_i = \sum_{k=1}^{2K} a_k e^{j\phi_k} e^{(-d_k + j\omega_k)(i-1)} = \sum_{k=1}^{2K} c_k w_k^{(i-1)}, \quad i = 1, \ldots, Q \tag{9}$$

where $j = \sqrt{-1}$. In Eq. (9), x_i represents the oscillation magnitude for $i = 1, \ldots, Q$, a_k is the amplitude of the kth sinusoidal component, d_k its damping factor, ω_k its angular frequency, and ϕ_k its initial phase. Note that damping factor d_k may be negative. In this case, the amplitude of the kth component grows with index i. $c_k = a_k e^{j\phi_k}$ is the complex-valued amplitude of the kth component, and $w_k = e^{(-d_k + j\omega_k)}$.

The observed signal segment $\mathbf{x} = [x_1, x_2, \ldots, x_Q]^T$ is entirely characterized by the parameters a_k, d_k, ω_k, ϕ_k, $k = 1, \ldots, 2K$. The number K of sinusoidal components can be estimated by MDL criterion [35].

3. Parameter estimation

In this section, we determine the parameters cited above by applying a variant of the parameter estimator in [21]. Firstly, we rearrange the signal segment $\mathbf{x}$ in a Hankel matrix of size $L \times M$ as follows:

$$\mathbf{X} = \begin{bmatrix} x_1 & x_2 & \ldots & x_M \\ x_2 & x_3 & \ldots & x_{M+1} \\ \vdots & \vdots & & \vdots \\ x_L & x_{L+1} & \ldots & x_Q \end{bmatrix} \tag{10}$$

where L, K, and Q are related by: $L \geq 2K$, $M \geq 2K$ and $Q = L + 2K - 1$.

Then, by implementing the Vandermonde Decomposition (VD) for Hankel data matrix of Eq. (10) with rank of $2K$, $\mathbf{X}$ can be written as

$$\mathbf{X} \overset{\text{VD}}{=} \mathbf{SCT}^T$$

where $\mathbf{C} = diag(c_1, c_2, \ldots, c_{2K})$

$$\mathbf{S} = \begin{bmatrix} 1 & 1 & \ldots & 1 \\ w_1^1 & w_2^1 & \ldots & w_{2K}^1 \\ \vdots & \vdots & & \vdots \\ w_1^{L-1} & w_2^{L-1} & \ldots & w_{2K}^{L-1} \end{bmatrix}$$

$$\mathbf{T}=\begin{bmatrix} 1 & 1 & \dots & 1 \\ w_1^1 & w_2^1 & \dots & w_{2K}^1 \\ \vdots & \vdots & & \vdots \\ w_1^{M-1} & w_2^{M-1} & \dots & w_{2K}^{M-1} \end{bmatrix}$$

According to the shift-invariant property in column space

$$\mathbf{S}^L=\mathbf{S}^F\mathbf{Z} \tag{11}$$

where $\mathbf{S}^L$ is a matrix containing all but the first rows of $\mathbf{S}$, and $\mathbf{S}^F$ is a matrix containing all but the last rows of $\mathbf{S}$. $\mathbf{Z}$ is a diagonal matrix whose nonzero terms depend on the expected parameters. By performing SVD, $\mathbf{X}$ can be decomposed as

$$\mathbf{X}\overset{\text{SVD}}{=}[\mathbf{U}_1 \quad \mathbf{U}_2]\begin{bmatrix} \boldsymbol{\Sigma}_1 & \mathbf{0} \\ \mathbf{0} & \boldsymbol{\Sigma}_2 \end{bmatrix}\begin{bmatrix} \mathbf{V}_1^H \\ \mathbf{V}_2^H \end{bmatrix} \tag{12}$$

where $(\cdot)^H$ is the Hermitian transposition, $\boldsymbol{\Sigma}_1$ contains the largest $2K$ singular values of $\mathbf{X}$ and $\boldsymbol{\Sigma}_2$ the $L-2K$ singular values of $\mathbf{X}$. The matrices $\mathbf{U}_1$ and $\mathbf{V}_1^H$ contain the first $2K$ left and right singular vectors, and their dimension is $L\times 2K$ and $M\times 2K$, respectively. Because the rank of $\mathbf{X}$ is $2K$, all values of $\boldsymbol{\Sigma}_2$ are null. Therefore, we can express $\mathbf{X}$ as

$$\mathbf{X}=\mathbf{U}_1\boldsymbol{\Sigma}_1\mathbf{V}_1^H \tag{13}$$

and we get the following equation from Eq. (11) by orthogonal basis transformation

$$\mathbf{U}_1^F\mathbf{Z}^u=\mathbf{U}_1^L \tag{14}$$

where $\mathbf{U}_1^F$ contains all but the last rows of matrix $\mathbf{U}_1$, $\mathbf{U}_1^L$ contains all but the first rows of matrix $\mathbf{U}_1$, and $\mathbf{Z}^u$ is a similarity transform of $\mathbf{Z}$. The damping factors d_k and frequencies ω_k $(k=1,\dots,2K)$ of the exponential sinusoidal model (see Eq. (9)) are estimated from the eigenvalues of $\mathbf{Z}^u$. Then we substitute these estimated d_k and ω_k in Eq. (9) and compute the least squares solution of the N linear equations. Finally, the amplitude a_k and phase ϕ_k of each component are determined from the magnitude and angle of c_k in Eq. (9). According to these estimated parameters, we can reconstruct the contour with its oscillations. The pixel coordinates in the contour are given as

$$\rho_i=r+\tilde{x}_i, \quad i=1,\dots,Q$$

where $\tilde{x}_i$ is the initial estimation of x_i, $i=1,\dots,Q$. To get closer to real-world conditions, we consider that the image is degraded by two sources of impairment: identically distributed white noise is added to the image, and/or the edge pixels are displaced randomly. The signal model of Eq. (9) becomes then

$$x_i'=x_i+n_i$$

So in the next section, we show how the signal can be refined to optimize the contour estimation.

4. Signal refinement

We get the initial estimation $\tilde{\mathbf{x}}$ from the previous section, which is the approximation of the original pixel oscillations. This estimation can be expressed as

$$\tilde{\mathbf{x}}=\mathbf{x}+\Delta\mathbf{x} \tag{15}$$

where $\Delta\mathbf{x}=[\Delta x_1,\Delta x_2,\dots,\Delta x_Q]^T$ is the perturbation vector contained in the initial estimation. Now, our aim is to minimize the norm of $\Delta\mathbf{x}$, *e.g.* $\|\Delta\mathbf{x}\|_2$, so that the final approximation is as close as possible to the original signals, while keeping $\tilde{\mathbf{x}}$ as a sum of $2K$ complex exponential sinusoids.

We rearrange the signal vector $\tilde{\mathbf{x}}$ in a Hankel matrix as

$$\tilde{\mathbf{X}}=[\tilde{\mathbf{X}}_L \quad \tilde{\mathbf{X}}_R] \tag{16}$$

where

$$\tilde{\mathbf{X}}_L=\begin{bmatrix} x_1 & x_2 & \dots & x_{2K-1} \\ x_2 & x_3 & \dots & x_{2K} \\ \vdots & \vdots & \vdots & \vdots \\ x_J & x_{J+1} & \dots & x_{Q-1} \end{bmatrix}, \quad \tilde{\mathbf{X}}_R=\begin{bmatrix} x_{2K} \\ x_{2K+1} \\ \vdots \\ x_Q \end{bmatrix}$$

and the number J of rows of Hankel matrix $\tilde{\mathbf{X}}$ should be greater than the number of signal components $2K$ while $J+2K=Q$.

Then $\tilde{\mathbf{X}}$ can be represented by the form similar to Eq. (15)

$$\tilde{\mathbf{X}}=[\mathbf{X}_L+\Delta\mathbf{X}_L \quad \mathbf{X}_R+\Delta\mathbf{X}_R]=[\mathbf{X}_L \quad \mathbf{X}_R]+[\Delta\mathbf{X}_L \quad \Delta\mathbf{X}_R]$$

where $[\mathbf{X}_L \quad \mathbf{X}_R]$ is a Hankel data matrix as the one in Eq. (10) and $[\Delta\mathbf{X}_L \quad \Delta\mathbf{X}_R]$ is a perturbation matrix, also with Hankel form.

Thus, we seek for the minimum norm of $[\Delta\mathbf{X}_L \quad \Delta\mathbf{X}_R]$ so that the approximation is the closest to the initial estimation, while the matrix $\tilde{\mathbf{X}}$ is rank-deficient, and matrices $[\mathbf{X}_L \quad \mathbf{X}_R]$ and $[\Delta\mathbf{X}_L \quad \Delta\mathbf{X}_R]$ have Hankel structure. This problem can be solved as the structured Total Least Norm problem by the iterative algorithm STLNB [32].

5. Experimental results

In this section, we apply the proposed method to test images and evaluate its performance. At the same time, we compare it with other methods, such as Hough transform [5] dedicated to circular-like contours, GVF (Gradient Vector Flow) method [8], and gradient optimization method following a specific signal generation scheme [13].

5.1. Parameter setup

In the simulations, the size of processed images is 100×100 pixels. We start by creating test images with a circular-like contour, where the contour center of gravity is set to be (50,50). An adequate number of sensors for the circular antenna is $Q=1600$. This elevated number of sensors is empirically chosen, and is relatively high because the expected contour may exhibit very concave contours. Indeed, for strongly concave contours, the pixel radial coordinates ρ_i vary much when the direction D_i of signal generation changes from sensor to sensor. To take into account all contour pixels in the generated signals, the number of sensors must be elevated. While estimating the number of sinusoidal components in the contour pixel coordinates, we run MDL criterion with the integer values 1–8 as set of candidates. Indeed MDL provides the accurate value as soon as this value is in the set of candidates, and we consider that eight sinusoids is by far enough to characterize a realistic strongly concave star-shaped contour. For the comparative methods Gradient and GVF, the parameters which best fit the expected contours and which are used in the experiments (unless specified) are the following: Gradient method [13] is run with step $\beta = 0.05$, and 150 iterations. GVF method is run as follows [8]. For the computation of the edge map: 100 iterations; $\mu_{GVF} = 0.09$ (regularization coefficient); for the snakes deformation: 100 initialization points and 400 iterations; $\alpha_{GVF} = 0.02$ (tension); $\beta_{GVF} = 0.03$ (rigidity); $\gamma_{GVF} = 1$ (regularization coefficient); $\kappa_{GVF} = 0.8$ (gradient strength coefficient). We define vectors $\mathbf{x}' = [x'_1, \ldots, x'_Q]^T$ and $\mathbf{x}'' = [x''_1, \ldots, x''_Q]^T$ as the first and second derivatives of edge curve vector $\mathbf{x}$, where x'_i and x''_i ($i = 1, \ldots, Q$) are the first and second derivative of edge curve vector $\mathbf{x}$ at the ith pixel. We use the finite differences to approximate the derivatives:

$x'_1 = 0$, and $\forall i = 2, \ldots, Q$ $x'_i = x_i - x_{i-1}$, and

$x''_1 = 0$, $\forall i = 2, \ldots, Q-1$ $x''_i = x_{i+1} - 2x_i + x_{i-1}$, and $x''_Q = x''_{Q-1}$.

We define the curvature of contour at each pixel location as follows:

$$\kappa_i = \frac{|x''_i|}{(1 + x'^2_i)^{3/2}}, \quad i = 1, \ldots, Q$$

The mean value of all $\kappa_i (i = 1, \ldots, Q)$ is computed by

$$\overline{\kappa} = \frac{1}{Q} \sum_{i=1}^{Q} \kappa_i$$

When the mean value $\overline{\kappa}$ is large, the contour is considered to be strongly concave.

The efficiency of the proposed method is measured by the mean error $ME_\mathbf{x}$ over the coordinates of the pixels of the contour. For the four quarters of an image, the coordinates of the pixels of the contour are contained in the vector $\mathbf{x} = [x_1, \cdots, x_Q]^T$ defined in Eq. (9), and their estimates are contained in vector $\hat{\mathbf{x}} = [\hat{x}_1, \ldots, \hat{x}_Q]^T$. The mean error value of the estimation for each trial is defined as

$$ME_\mathbf{x} = \frac{1}{Q} \sum_{i=1}^{Q} |\hat{x}_i - x_i|$$

where $|\cdot|$ means absolute value. So for J trials, the mean error on pixel position is given by

$$ME = \frac{1}{J} \sum_{j=1}^{j=J} ME_{\mathbf{x}_j}$$

where $ME_{\mathbf{x}_j}$ is the mean error value corresponding to the jth trial.

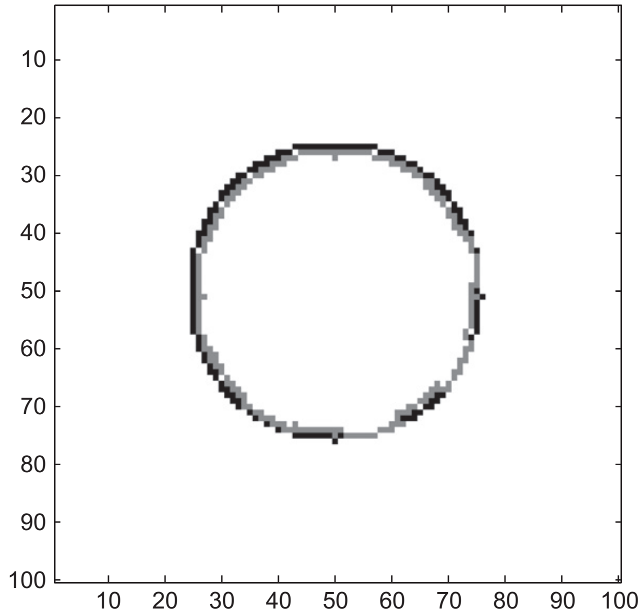

Fig. 5. Circle: superposition expected contour and result obtained by the proposed method: $ME_\mathbf{x} = 1.71$.

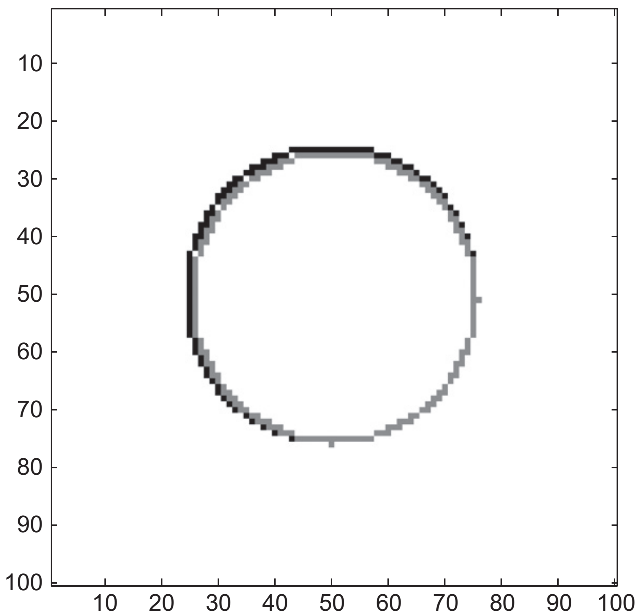

Fig. 4. Circle: superposition expected contour and result obtained by Hough method: $ME_\mathbf{x} = 1.65$.

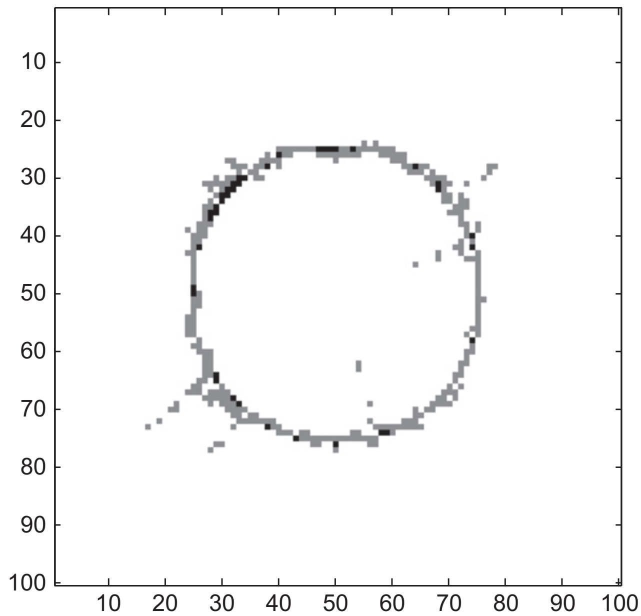

Fig. 6. Circle: superposition expected contour and result obtained by Gradient method: $ME_\mathbf{x} = 3.24$.

To evaluate the robustness of the methods, the root mean squared error (*RMSE*) of pixel bias is also used and defined as follows:

$$RMSE = \sqrt{\frac{1}{J}\sum_{j=1}^{j=J} |ME_{\mathbf{x}_j} - ME|^2}$$

• *Experiment* 1: *circular-like contour*: In this experiment, we construct a nearly circular star-shaped contour, and add Gaussian white noise in images with mean value 0 and standard deviation 1, to compare our method with the Hough transform, Gradient and GVF methods. The number K of sinusoids estimated by MDL is 1. From Figs. 4–7, where the result contour is plotted in gray, it can be seen that all four methods detect the contour with a rather low bias: values of mean error $ME_{\mathbf{x}}$ are 1.65, 1.71, 3.24 and 1.85 pixels respectively. The number of iterations is 60 for Gradient method and 200 for GVF method.

• *Experiment* 2: *case of small/large edge oscillations*: In some cases, due to the acquisition conditions or the image quantization, the continuous form of contour edge is not perfect. It is therefore very interesting to evaluate the robustness of the proposed method to pixel location errors. We produce test images by initially creating a star-shaped contour and then adding pixel displacement by modifying the actual pixel radial coordinates with a

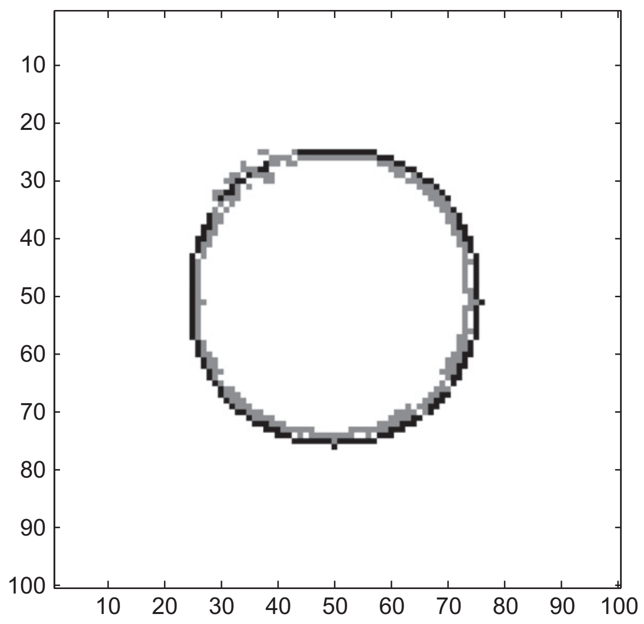

Fig. 7. Circle: superposition expected contour and result obtained by GVF method: $ME_{\mathbf{x}} = 1.85$.

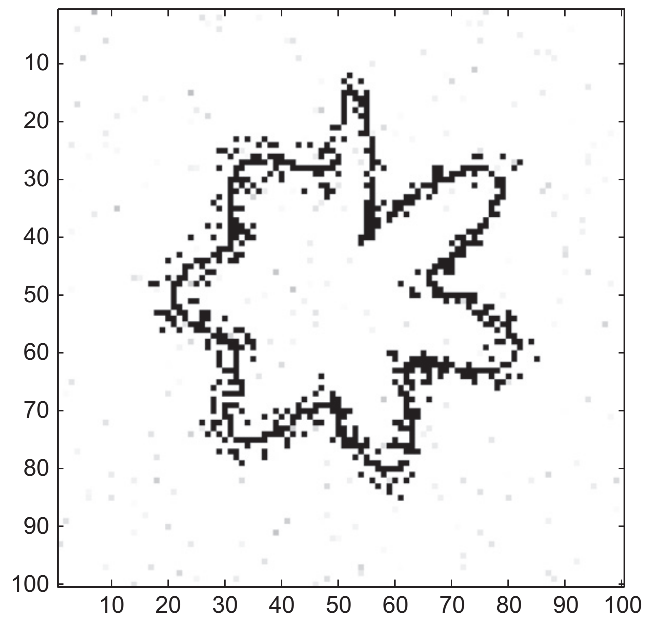

Fig. 9. Processed image, with large edge perturbation and noise $(0,10^{-2})$.

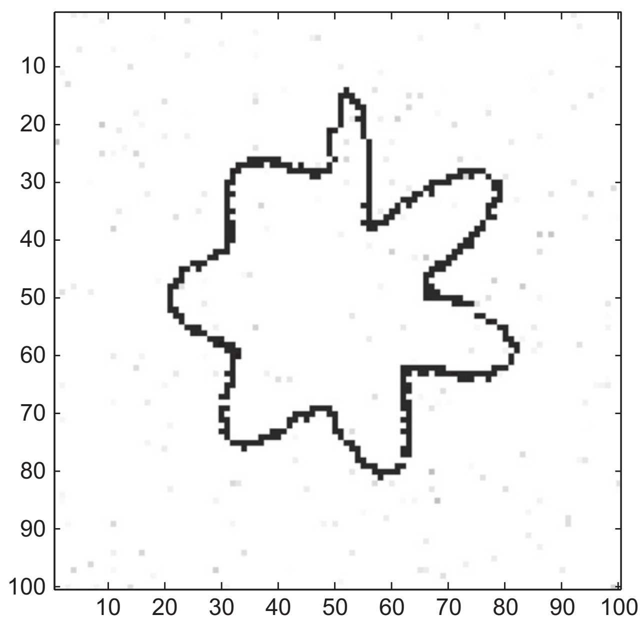

Fig. 8. Processed image: $\overline{\kappa} = 2.7 \times 10^{-3}$, with small edge perturbation and noise $(0,10^{-2})$.

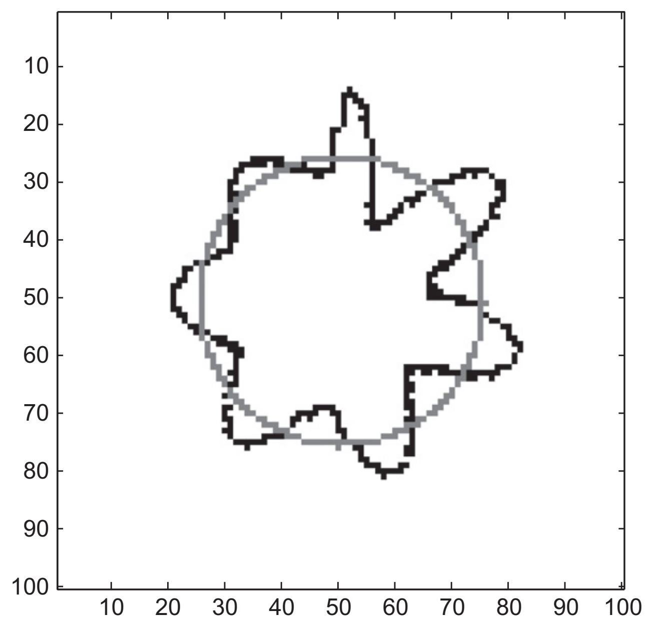

Fig. 10. Initialization of the methods for both processed images of Figs. 8 and 9.

Gaussian random variable. Either with mean value 0 and standard deviation 1 (see Fig. 8), or with mean value 3 and standard deviation 2 (see Fig. 9). The pixel coordinates are rounded to the nearest integer. We assume there exists equally distributed random noise in the image, with mean value 0 and standard deviation 10^{-2}. The number K of sinusoids estimated by MDL is 3 (Fig. 10). Referring to Figs. 11–16, when the proposed method is applied, the mean error is $ME_{\mathbf{x}} = 1.61$ when small random displacements are added; and $ME_{\mathbf{x}} = 1.86$ when larger random displacements are added. When Gradient method is applied, the mean error value is increased dramatically from $ME_{\mathbf{x}} = 1.78$ to $ME_{\mathbf{x}} = 2.25$. When GVF is applied, the mean error value is increased from $ME_{\mathbf{x}} = 1.90$ to $ME_{\mathbf{x}} = 2.42$. So, Figs. 11–16 show that the proposed method is not sensitive to the random pixel displacements, contrary to Gradient method and GVF method. This is due to the fact that the proposed method processes the signal generated from the image as a whole, providing parameters of interest, whereas Gradient method and GVF are local methods, which may focus on random pixels.

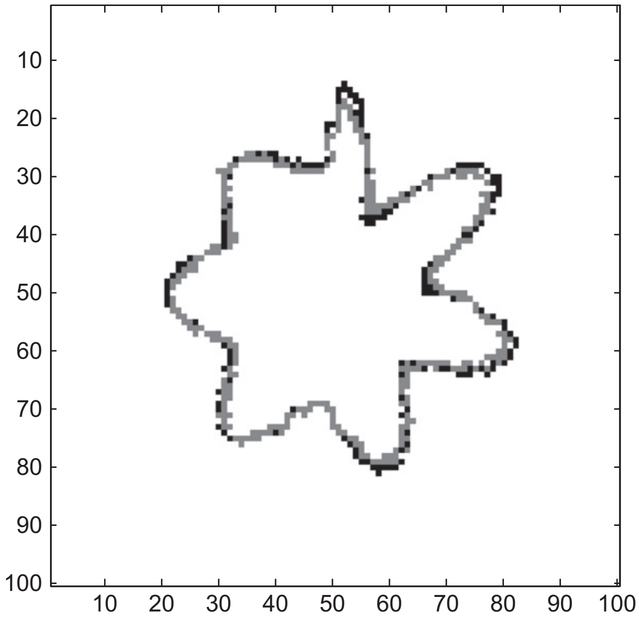

Fig. 11. Superposition processed and result obtained from Fig. 8 by the proposed method ($ME_{\mathbf{x}} = 1.58$).

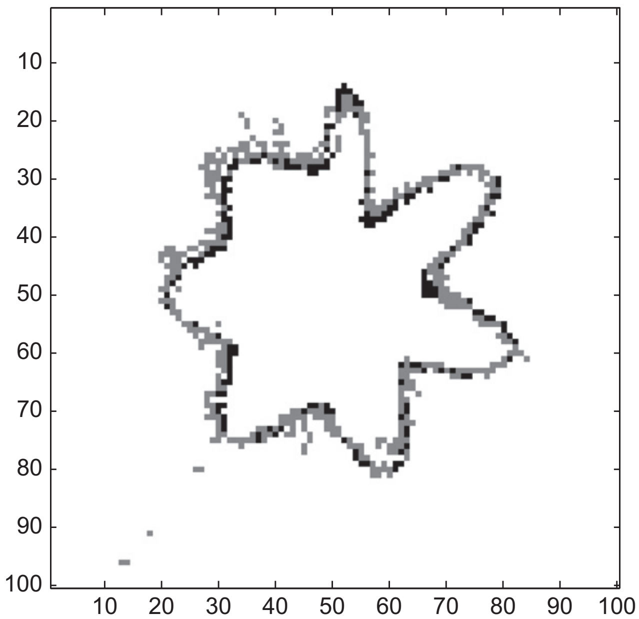

Fig. 12. Superposition processed and result obtained from Fig. 8 by Gradient method ($ME_{\mathbf{x}} = 1.78$).

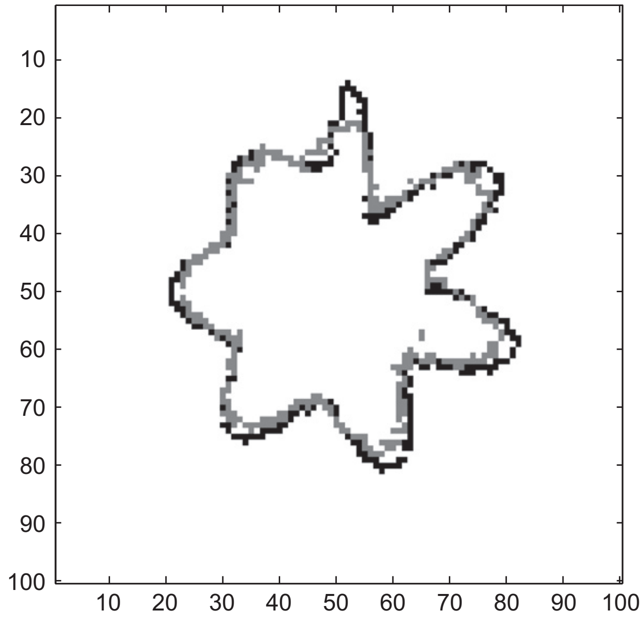

Fig. 13. Superposition processed and result obtained from Fig. 8 by GVF method ($ME_{\mathbf{x}} = 1.90$).

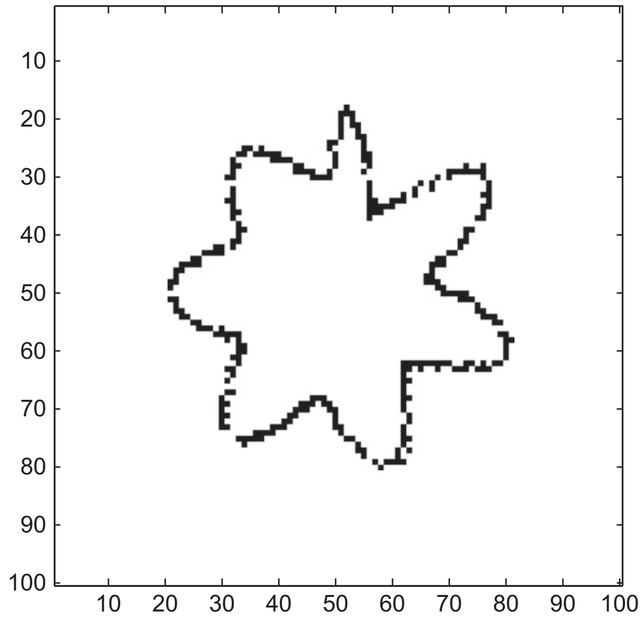

Fig. 14. Superposition processed and result obtained from Fig. 9 by the proposed method ($ME_{\mathbf{x}} = 1.86$).

- *Experiment* 3: *sensitivity to background noise and strong contour concavity*: We now consider a contour with

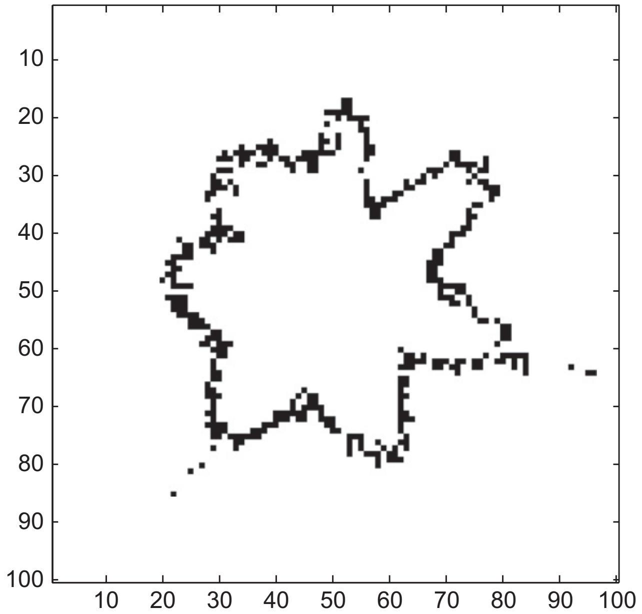

Fig. 15. Superposition processed and result obtained from Fig. 9 by Gradient method ($ME_{\mathbf{x}} = 2.25$).

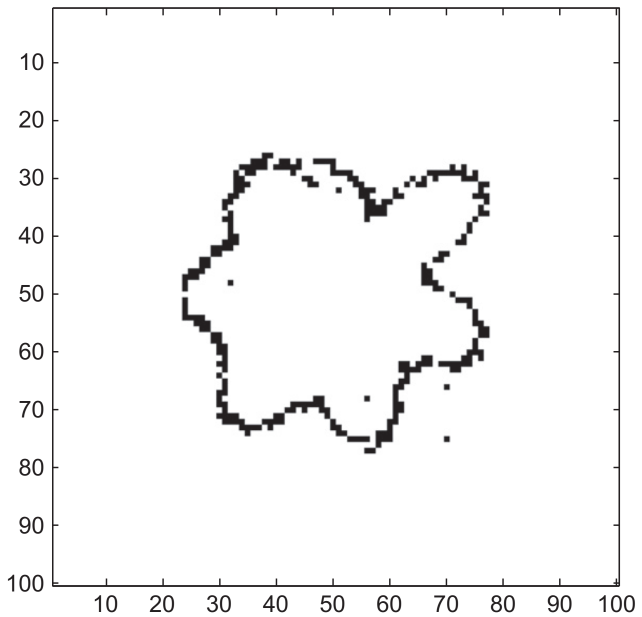

Fig. 16. Superposition processed and result obtained from Fig. 9 by GVF method ($ME_{\mathbf{x}} = 2.42$).

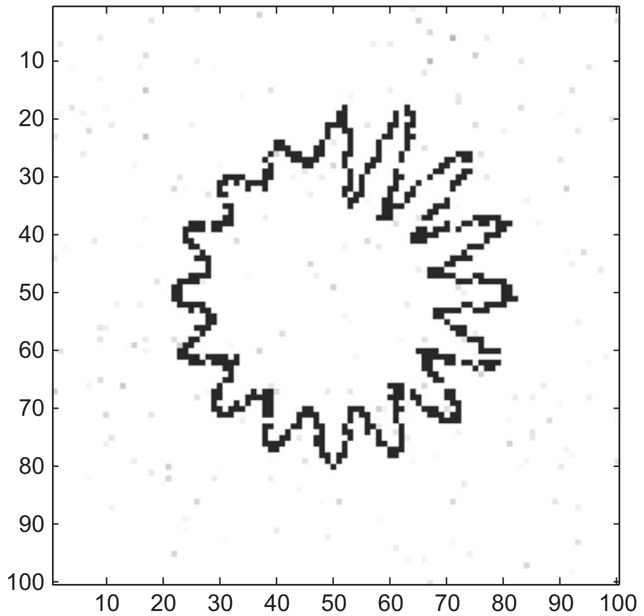

Fig. 17. Processed image with contour concavity $\overline{\kappa} = 1.17 \times 10^{-2}$ and noise parameters $(0,10^{-2})$.

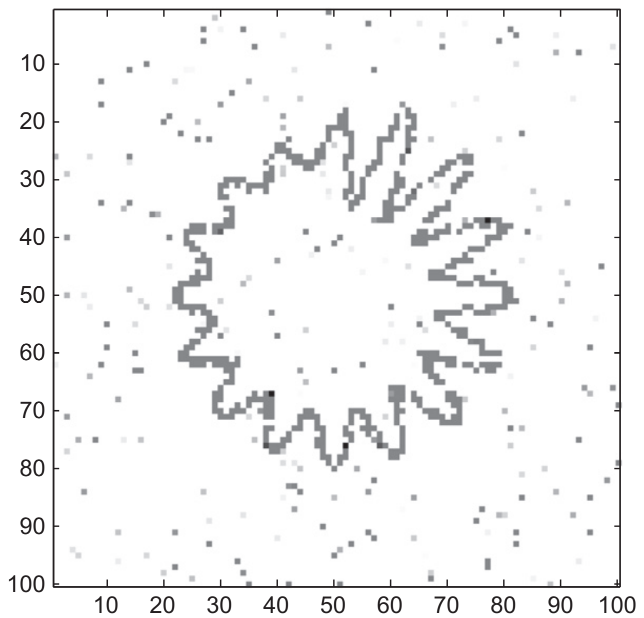

Fig. 18. Processed image with same contour as in Fig. 17 and noise parameters (0,1).

stronger concavity. Fig. 17 shows the noisy processed image. The noise mean value and standard deviation are 0 and 10^{-2} (see Fig. 18). The initial estimated radius obtained from Eq. (7) is 30 (see Fig. 19). The number K of sinusoids estimated by MDL is 3. Figs. 20 and 23 show the results obtained by the proposed method, which match well the expected contour, though the contour concavity is strong and the noise level is elevated. From the least to the most noisy image, the mean pixel bias changes just from 1.61 to 1.86. From Figs. 21, 22, 24 and 25, we get that Gradient method and GVF method (run with 100 and 500 iterations respectively) do not converge very well to the expected contour. After increasing the noise level, the mean error values increase from $ME_{\mathbf{x}} = 1.80$ to $ME_{\mathbf{x}} = 4.02$ when Gradient is run, and from $ME_{\mathbf{x}} = 3.17$ to $ME_{\mathbf{x}} = 3.21$ when GVF is run. This proves that our method performs better than Gradient method and GVF method for a strongly concave contour with either low or high level noise, and that Gradient method is very sensitive to the noise level, whereas GVF method does not cope with a contour with strong concavity. Note that, considering the

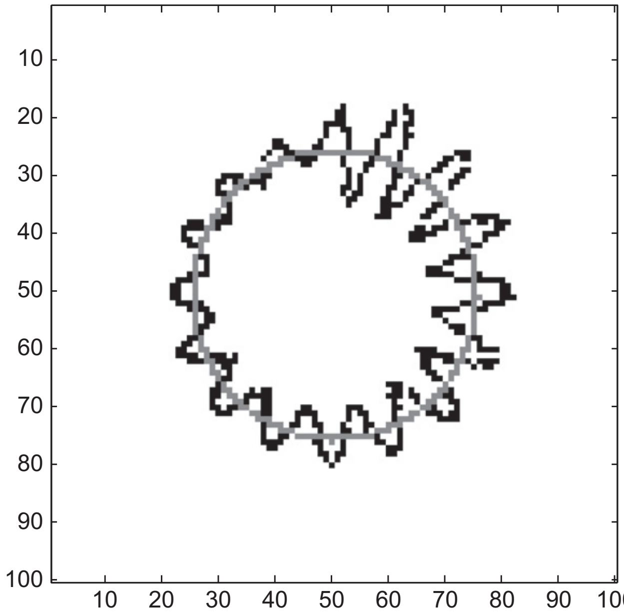

Fig. 19. Superposition expected contour and initialization circle for both processed images of Figs. 17 and 18.

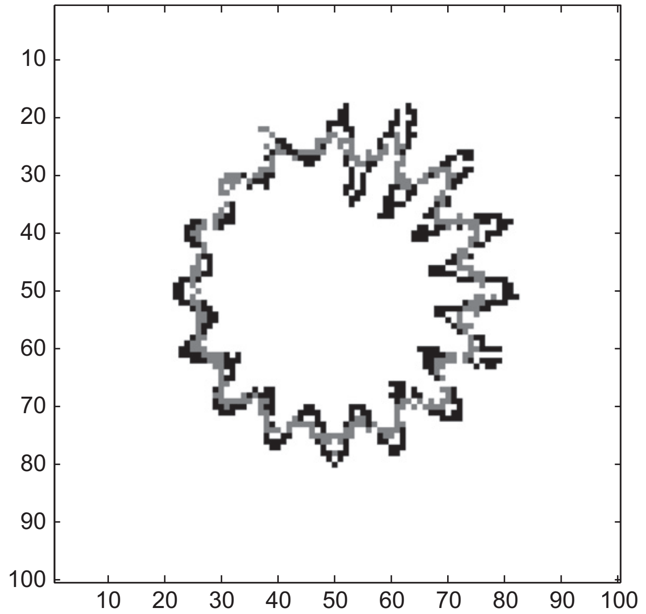

Fig. 21. Superposition expected contour and result obtained from Fig. 17 by Gradient method ($ME_{\mathbf{x}} = 1.80$).

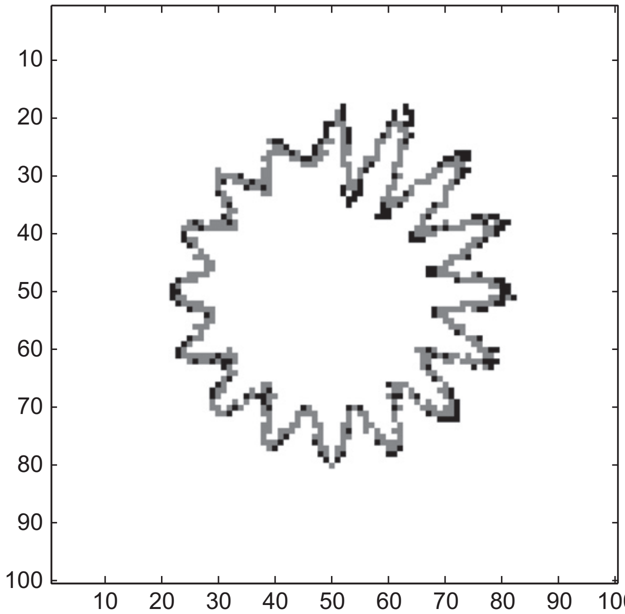

Fig. 20. Superposition expected contour and result obtained from Fig. 17 by the proposed method ($ME_{\mathbf{x}} = 1.61$).

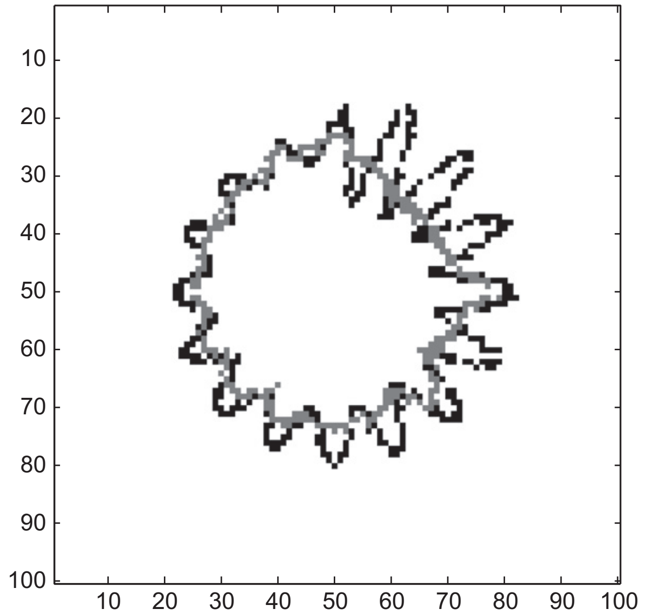

Fig. 22. Superposition expected contour and result obtained from Fig. 17 by GVF ($ME_{\mathbf{x}} = 3.17$).

computational load and the accuracy of estimation for Gradient method and GVF method, we may choose different iteration times for different levels of concavity. We choose the number of iterations so that the accuracy of the result is not significantly improved when the number of iterations is increased.

The values of mean error with different levels of noise and contour concavity are presented in Table 1, where the first case corresponds to the curvature 0, that means, the contour is a circle as in Figs. 3–7, and the last case corresponds to the strongly concave contour as in Figs. 17–25. Each experiment is repeated 50 times with a different noise realization. It shows that:

- the proposed method is insensitive to both noise level and contour concavity;
- the GVF method is sensitive to contour concavity;
- the Gradient method is sensitive to noise.

At the same time, we see that when noise variance is reduced, the accuracy of estimation for all methods is improved.

Table 1
ME values (in pixel) obtained with the proposed method (value with refinement/without refinement) (A), Gradient method (B) and GVF method (C), versus concavity and noise percentage.

Concavity $\overline{\kappa}$	Noise					
	$(0{,}10^{-3})$			$(10^{-2},\ 10^{-2})$		
	(A)	(B)	(C)	(A)	(B)	(C)
0	0.12	0.68	0.19	0.16	0.99	0.20
2.2×10^{-3}	0.13	0.69	0.21	0.15	0.97	0.24
2.7×10^{-3}	0.17	0.76	0.30	0.19	1.03	0.32
1.17×10^{-2}	0.20	0.75	0.45	0.21	1.15	0.49
Concavity $\overline{\kappa}$	Noise					
	$(0{,}10^{-1})$			$(0{,}1)$		
	(A)	(B)	(C)	(A)	(B)	(C)
0	0.24	1.32	0.19	0.30	1.44	0.21
2.2×10^{-3}	0.27	1.40	0.29	0.34	1.37	0.28
2.7×10^{-3}	0.31	1.55	0.33	0.45	1.59	0.33
1.17×10^{-2}	0.52	1.83	0.48	0.59	2.25	0.51

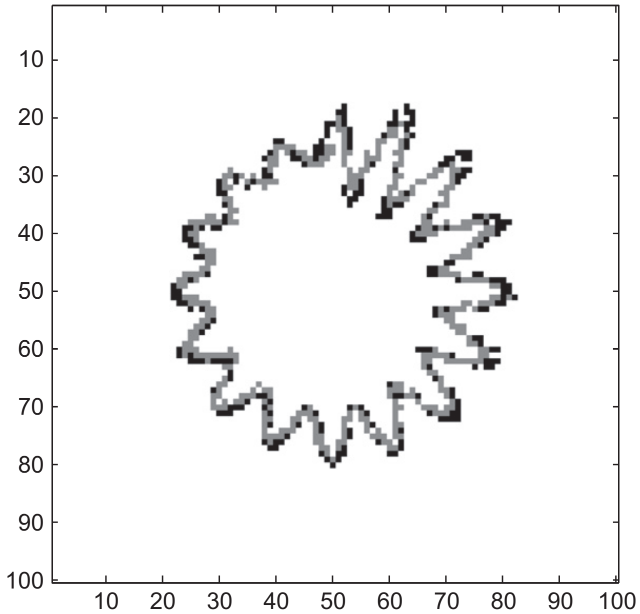

Fig. 23. Superposition expected contour and result obtained from 18 by the proposed method ($ME_{\mathbf{x}} = 1.86$).

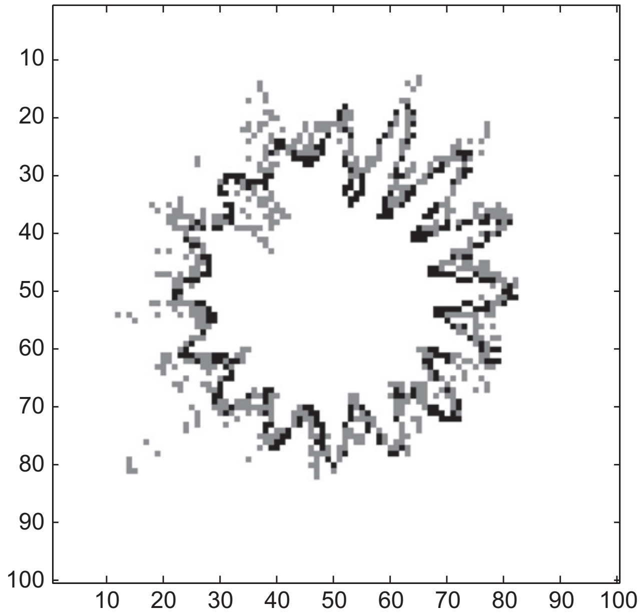

Fig. 24. Superposition expected contour and result obtained from 18 by Gradient method ($ME_{\mathbf{x}} = 4.02$).

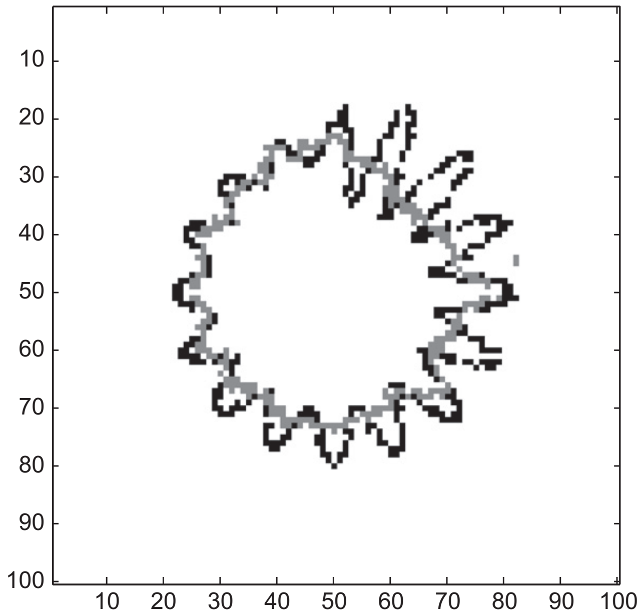

Fig. 25. Superposition expected contour and result obtained from 18 by GVF ($ME_{\mathbf{x}} = 3.21$).

With different levels of noise and contour concavity, the values of RMSE are shown in Table 2. It can be seen that the proposed method always yields small RMSE values, which means that the proposed method is robust to the contour concavity and the noise level. As seen from Tables 1 and 2, the proposed method has the best performance in both accuracy and robustness, followed by GVF method and Gradient method.

To evaluate the computational load of proposed method, each method is run 50 times on a PC with 2 Quad CPU 2.83 GHz and 4 Gb memory. Whatever the concavity strength and the noise parameters, the average elapsed time is 1.098 s to detect the parameters of the damped exponential sinusoid model, and it needs 60.91 s to refine the signals when the noise level is elevated. When the noise level is very low, it is not necessary to adopt the refinement of the signals: with noise parameters $(0{,}10^{-3})$ and $(10^{-2}{,}10^{-2})$, the improvement is around 1%. When the noise level is higher, that is, with noise parameters $(0{,}10^{-1})$ and (0,1), the improvement is around 4% and 16% respectively. The accuracy of the estimation depends essentially on the adequate signal generation and the damped frequency estimation method. Depending on the application, one may want to refine the signals at the expense of a higher computational load.

Table 2
RMSE values (in pixel) obtained with the proposed method (A), Gradient method (B) and GVF method (C), versus concavity and noise percentage.

Concavity $\overline{\kappa}$	Noise					
	$(0,10^{-3})$			$(10^{-2}, 10^{-2})$		
	(A)	(B)	(C)	(A)	(B)	(C)
0	1.49/1.50	1.52	1.70	1.53/1.55	1.76	1.70
2.2×10^{-3}	1.53/1.54	1.55	1.79	1.54/1.55	1.81	1.78
2.7×10^{-3}	1.57/1.58	1.59	1.91	1.59/1.60	1.79	1.92
1.17×10^{-2}	1.58/1.60	1.66	3.29	1.63/1.65	1.84	3.30
Concavity $\overline{\kappa}$	Noise					
	$(0,10^{-1})$			$(0,1)$		
	(A)	(B)	(C)	(A)	(B)	(C)
0	1.60/1.72	2.21	1.70	1.67/1.91	3.64	1.71
2.2×10^{-3}	1.68/1.74	2.27	1.79	1.69/1.98	3.87	1.80
2.7×10^{-3}	1.75/1.78	2.46	1.92	1.78/2.00	3.93	1.93
1.17×10^{-2}	1.89/1.97	2.83	3.27	1.96/2.35	4.15	3.29

Concerning Gradient algorithm: as soon as the noise variance is higher than 10^{-2}, Gradient method does not provide satisfying results (see for instance Fig. 24); then we provide the computational load when noise parameters are $(0,10^{-3})$: for concavity 2.2×10^{-3}, Gradient method needs 0.11 s for 150 iterations. For concavity 1.17×10^{-2}, Gradient method needs 0.22 s for 300 iterations. So Gradient is faster than the proposed methods, but breaks down as soon as the noise is slightly elevated, which is a drawback for any real-world application. GVF does not provide satisfying results for concavity values which are higher than 2.5×10^{-3}. For concavity 2.2×10^{-3}, and noise parameters $(0,10^{-3})$, GVF requires 1.989 s for 400 iterations. For concavity 2.2×10^{-3}, and noise parameters $(0,10^{-3})$, GVF requires 2.020 s for 400 iterations. When the refinement step is not needed, our method presents the following advantage: we do not need to specify any *a priori* known number of iterations. Contrary to the two comparative methods, the proposed method works in both harsh conditions: strong concavity and high noise level. Moreover, it exhibits the same computational load whatever the experimental conditions: concavity and noise level. In the considered conditions, this computational load is two times lower than for GVF.

6. Conclusion

Strongly concave contours are characterized, based on a damped sinusoid model, which fits signals generated out of the processed image: an adequate transformation of the image content provides a 1-D signal, which can be exploited to retrieve the polar coordinates of the contour pixels. A frequency estimation method yields the amplitude, frequency, damping factor and phase of the damped sinusoids which compound the oscillations in pixel positions around a circle which best fits the expected contour. Furthermore, we additionally refine the generated signals by STLNB optimization method so that they better fit the proposed model, in order to improve the estimation when the noise level is high. The proposed methods are applied to test images to evaluate their performance. It has been shown that there is a significant improvement with respect to comparative methods in terms of pixel bias, especially when the contour concavity is strong and the noise level is high.

References

[1] J.F. Canny, A computational approach to edge detection, IEEE Transactions on PAMI 8 (6) (1986) 679–698.
[2] W. Frei, C. Chen, Fast boundary detection: a generalization and a new algorithm, IEEE Transactions on Computers 26 (2) (1977) 988–998.
[3] T. Folsom, R. Pinter, Primitive features by steering, quadrature and scale, IEEE Transactions on PAMI 20 (11) (1998) 1161–1173.
[4] P. Perona, J. Malik, Scale-space and edge detection using anisotropic diffusion, IEEE Transactions on PAMI 12 (7) (1990) 629–639.
[5] D.H. Ballard, Generalizing the Hough transform to detect arbitrary shapes, Pattern Recognition 13 (2) (1981) 111–122.
[6] J.A. Sethian, Level Set Methods and Fast Marching Methods, Cambridge University Press, New York, 1999.
[7] C. Li, C. Xu, Distance regularized level set evolution with application to image segmentation, IEEE Transactions on IP 19 (12) (2010) 3243–3254.
[8] C. Xu, J.L. Prince, Snakes, shapes, and gradient vector flow, IEEE Transactions on IP 7 (3) (1998) 359–369.
[9] M.-A. Charmi, S. Derrode, F. Ghorbel, Fourier-based geometric shape prior for snakes, Pattern Recognition Letters 29 (7) (2008) 897–904.
[10] T. Lei, J. Udupa, A sensor array processing approach to object region detection, IEEE Transactions on BE 48 (11) (2001) 1319–1325.
[11] P. Milanfar, G. Verghese, W. Karl, A. Willsky, Reconstructing polygons from moments with connections to array processing, IEEE Transactions on SP 43 (2) (1995) 432–443.
[12] H.K. Aghajan, T. Kailath, Sensor array processing techniques for super resolution multi-line-fitting and straight edge detection, IEEE Transactions on IP 2 (4) (1993) 454–465.
[13] J. Marot, S. Bourennane, Subspace-Based and DIRECT algorithms for distorted circular contour estimation, IEEE Transactions on IP 16 (9) (2007) 2369–2378.
[14] M. Viberg, Subspace fitting concepts in sensor array processing, Signal Processing 19 (4) (1990) 345.
[15] T. Trump, B. Ottersten, Estimation of nominal direction of arrival and angular spread using an array of sensors, Signal Processing 50 (1–2) (1996) 57–69.
[16] H. Chen, J. Zhao, Coherent signal-subspace processing of acoustic vector sensor array for DOA estimation of wideband sources, Signal Processing 85 (4) (2005) 837–847.
[17] M.A. Hasan, DOA and frequency estimation using fast subspace algorithms, Signal Processing 77 (1) (1999) 49–62.

[18] S. Bourennane, C. Fossati, J. Marot, About noneigenvector source localization methods, EURASIP Journal on Advances in Signal Processing (2008) 1–13 Article ID 480835.

[19] F. Gini, M. Montanari, L. Verrazzani, Maximum likelihood, ESPRIT, and periodogram frequency estimation of radar signals in K-distributed clutter, Signal Processing 80 (6) (2000) 1115–1126.

[20] M.A. Altinkaya, H. Deliç, B. Sankur, E. Anarim, Subspace-based frequency estimation of sinusoidal signals in alpha-stable noise, Signal Processing 82 (12) (2002) 1807–1827.

[21] H. Chen, S. Van Huffel, A. Van den Boom, P. Van den Bosch, Subspace-based parameter estimation of exponentially damped sinusoids using prior knowledge of frequency and phase, Signal Processing 59 (1) (1997) 129–136.

[22] J.R. Deller Jr., J.H. Hansen, J.G. Proakis, Discrete-Time Processing of Speech Signals, IEEE Computer Society Press, 1999.

[23] J. Jensen, S.H. Jensen, E. Hansen, Exponential sinusoidal modeling of transitional speech segments, Proceedings of ICASSP'99 1 (March) (1999) 473–476.

[24] R.O. Schmidt, Multiple emitter location and signal parameters estimation, IEEE Transactions on ASSP 4 (3) (1983) 276–280.

[25] R. Roy, T. Kailath, ESPRIT—Estimation of signal parameters via rotational invariance techniques, IEEE Transactions on ASSP 37 (7) (1989) 984–995.

[26] M. Elad, P. Milanfar, G.H. Golub, Shape from moments—an estimation theory perspective, IEEE Transactions on SP 52 (7) (2004) 1814–1829.

[27] M. Schumermans, P. Lemerling, L. De Lathauwer, S. Van Huffel, The use of total least squares data fitting in the shape-from-moments problem, Signal Processing 86 (5) (2006) 1109–1115.

[28] S. Bourennane, J. Marot, Estimation of straight line offsets by a high-resolution method, IEE Vision Image and Signal Processing 153 (2) (2006) 224–229.

[29] H. Jiang, J. Marot, C. Fossati, S. Bourennane, Fuzzy contour characterization by subspace based methods of array processing and direct method, in: Proceedings of EUSIPCO 2010, 2010, pp. 1344–1348.

[30] H. Jiang, J. Marot, C. Fossati, S. Bourennane, Fuzzy triangle contour characterization by subspace based methods of array processing, in: Proceedings of IEEE Workshop on Sensor Array and Multi-channel Signal Processing, Israël, October 2010, pp. 165–168.

[31] J. Marot, S. Bourennane, Array processing and fast optimization algorithms for distorted circular contour retrieval, EURASIP Journal on Advances in Signal Processing (2007) 1–13 Article ID 57354.

[32] S. Van Huffel, H. Park, J.B. Rosen, Formulation and solution of structured total least norm problems for parameter estimation, IEEE Transactions on SP 44 (October) (1996) 2464–2474.

[33] R. Takiyama, N. Ono, A least square error estimation of the center and radii of concentric arcs, Pattern Recognition Letters 10 (4) (1989) 237–242.

[34] J. Borkowski, B.J. Matuszewski, J. Mroczka, L.-K. Shark, Geometric matching of circular features by least-squares fitting, Pattern Recognition Letters 23 (7) (2002) 885–894.

[35] M. Wax, T. Kailath, Detection of signals by information theoretic criteria, IEEE Transactions on ASSP 33 (2) (1985) 387–392.